2014 IEEE International Conference on Systems, Man, and Cybernetics
October 5-8, 2014, San Diego, CA, USA

Muscle and Electrode Motion Artifacts Reduction in ECG Using Adaptive Fourier Decomposition

Ze Wang, Chi Man Wong, Janir Nuno da Cruz, Feng Wan, Pui-In Mak, Peng Un Mak and Mang I Vai
Department of Electrical and Computer Engineering, Faculty of Science and Technology, University of Macau
Email: db02906@umac.mo, chiman465@gmail.com, mb35436@umac.mo, fwan@umac.mo

***Abstract*—The reduction of the muscle and electrode motion artifacts in ECG using the adaptive Fourier decomposition (AFD) is investigated. This is an extension of our previous work, in which AFD is first proposed for ECG denoising and its effectiveness in filtering out the additive Gaussian white noise is tested. This paper studies the AFD-based ECG denoising method for two types of ECG noise due to the electrode movement and the muscle contraction which are common and important in practice. In addition, some rules on the selection and adjustment of the AFD decomposition level are proposed. The tests on the MIT-BIH Arrhythmia Database indicate that this AFD-based denoising scheme performs better than the Butterworth lowpass filter, the wavelet transform and the empirical mode decomposition methods for ECG denoising with the muscle movement and electrode motion artifacts.**

***Index Terms*—ECG signal denoising, adaptive Fourier decomposition, muscle artifact, electrode motion artifact**

I. Introduction

The electrocardiogram (ECG) signal is the electrical interpretation of the heart activity. Usually, the ECG signal is weak and buried in noises, due to the electrode motion and muscle contraction for instance, which are very difficult to be filtered out from the ECG signals. Therefore, it is necessary to have a suitable denoising method for real ECG noise reduction. Until now, some linear and nonlinear denoising methods of the ECG signals have been proposed. Linear denoising methods are traditional methods of the ECG denoising. However, since the frequency spectrums of the noise and ECG signals usually overlap each other, linear denoising methods based on the frequency analysis may damage original ECG signals. Furthermore, ECG signals are often non-stationary and thus linear denoising methods may not be suitable and effective. To overcome these disadvantages, several nonlinear approaches were reported. Among them, the wavelet-based methods are widely used since they are suitable for the denoising of the Gaussian noise [1–5]. However, there are two significant problems of this type of methods. First, the filtered results of wavelet-based methods depend on the choice of the mother wavelets. Finding a suitable mother wavelet that can always provide good filtered results is difficult. Second, the wavelet transform may lead to oscillations in the reconstructed ECG signals or the amplitude decreases of the ECG waveforms [5]. In order to solve these two problems, the ECG denoising method based on the empirical mode decomposition (EMD) is proposed [6, 7]. The main technique of the denoising method based on the EMD is to decompose the noisy signal into some intrinsic mode functions (IMFs), then remove the IMFs containing most noise and finally reconstruct the signal with remaining IMFs. Since the decomposition is based on the local characteristics of the data, the basis function of the EMD can be derived automatically. In addition, the EMD has good localization properties [8]. Therefore, the oscillation problem does not exist in its reconstructed signals. However, this method does not have an explicit mathematical explanation. In practice, it is difficult to understand and interpret its decomposition results. Moreover, in some cases, analytic phase functions of IMFs are not monotone [9]. In other words, a physically meaningful analytic instantaneous frequency of IMFs cannot be defined in generally. In addition, IMFs may have negative phase derivatives in practice, which will affect the analysis of the decomposition results based on the EMD and the threshold judgment [8].

To overcome these disadvantages of the wavelet transform and the EMD, a novel signal decomposition method called adaptive Fourier decomposition (AFD) was introduced by Qian et al [10, 11]. The AFD is based on the sequential extraction of energy starting from the high-energy mode to the low-energy mode. The total summation of mono-components matches the original signal, thus ensuring the completeness of the original signal. The AFD presents three major advantages when compared to the wavelet transform and the EMD: the basis functions are fixed to the signal automatically; all decomposition results are mono-components whose analytic phase derivatives are non-negative; it has a rigorous mathematical foundation [10]. However, the most difficult problem of the AFD is how to find the suitable decomposition level to filter out the noise and retain the original ECG signal. In our previous work [12], a judgment based on the estimated signal-to-noise ratio (SNR) of the noisy ECG signals is proposed to stop the recursive AFD process when enough mono-components have been obtained. In addition, the effectiveness of the AFD-based denoising method for the reduction of the additive Gaussian white noise was shown through the tests on the MIT-BIH Arrhythmia Database. For the ECG denoising, it is not enough by only considering such a simple and ideal case.

In this paper, we use the AFD with the estimated-SNR-based judgment to filter out noises caused by the muscle contraction and the electrode motion, which is more realistic to show that the proposed AFD-based denoising method is a promising tool for the ECG signal denoising. Moreover, some rules about how to choose and adjust the decomposition level

978-1-4799-3840-7/14/$31.00 ©2014 IEEE

to get the optimal denoising results are introduced.

II. Adaptive Fourier Decomposition

The AFD involves the adaptive decomposition of a given signal $G(t)$ that is in $H^2(\partial\mathbb{D})$ space where $\mathbb{D} = \{z \in \mathbb{C} : |z| < 1\}$ and $\mathbb{C}$ is the complex plane into a series of mono-components. After the AFD, $G(t)$ is decomposed into a summation of a series of mono-components $s_n(t)$'s and a standard remainder $R_N(t)$ shown in (1). In practice, most real signals $s(t)$'s are in $L^2(\partial\mathbb{D})$ space. According to the relationship shown in (2) where f and f^+ are signals in $L^2(\partial\mathbb{D})$ space and $H^2(\partial\mathbb{D})$ space, it is possible to reconstruct the real signal $s(t)$ by only using $G(t)$.

$$G(t) = \sum_{k=0}^{\infty} c_k e^{jkt} = \sum_{n=1}^{N} s_n(t) + R_N(t), \ \sum_{k=0}^{\infty} |c_k|^2 < \infty \quad (1)$$

$$f = \sum_{k=-\infty}^{\infty} c_k e^{jkt} = 2\,\mathrm{Re}\left\{f^+\right\} - c_0, \ \sum_{k=-\infty}^{\infty} |c_k|^2 < \infty \quad (2)$$

The AFD use the rational orthogonal system, or the Takenaka-Malmquist system, $\{B_n\}_{n=1}^{\infty}$, as its basis functions where

$$B_n(e^{jt}) = \frac{\sqrt{1-|a_n|^2}}{1-\overline{a}_n e^{jt}} \prod_{k=1}^{n-1} \frac{e^{jt}-a_k}{1-\overline{a}_k e^{jt}}, \quad (3)$$

$a_n \in \mathbb{D}$, $n = 1, 2, \cdots$ [11]. For $B_n(e^{jt})$, there are two points that should be noted. First, in (3), $\frac{e^{jt}-a_k}{1-\overline{a}_k e^{jt}}$ is a complex number. In addition, its amplitude is equal to 1 for any e^{jt}. Therefore, $B_n(e^{jt})$ can be represented as [13]

$$B_n(e^{jt}) = \rho_n(t) e^{j\phi_n(t)}. \quad (4)$$

Second, characteristics of $B_n(e^{jt})$ are related with a_n. As we have mentioned, to make sure that all decomposition results have physically meaningful phase derivatives, decomposition results of the AFD should be in $H^2(\partial\mathbb{D})$ space. This goal can be achieved by finding a suitable array $\{a_1, a_2, \cdots, a_n\}$ to make sure that $\phi_n(t)$ in (4) is always positive. To increase the speed of convergency, the array $\{a_1, a_2, \cdots, a_n\}$ also needs to keep standard remainders $R_N(t)$'s minimum for every steps. The main purpose of the AFD is to find such kind of array $\{a_1, a_2, \cdots, a_n\}$ that is able to achieve these two goals.

In the algorithm of the AFD, all mono-components are found one by one in the energy point of view. The AFD extracts mono-components from the high-energy mode to the low-energy mode sequentially. To find energy relationship easily, reduced remainders G_n's are defined by using their corresponding standard remainders R_{n-1}'s [10]:

$$G_n(e^{jt}) = R_{n-1}(e^{jt}) \prod_{l=1}^{n-1} \frac{1-\overline{a}_l e^{jt}}{e^{jt}-a_l}. \quad (5)$$

Then (1) can be expressed by using reduced remainders G_n's:

$$G(t) = \sum_{n=1}^{N} \left\langle G_n, e_{\{a_n\}} \right\rangle B_n(e^{jt}) + G_{N+1}(e^{jt}) \prod_{n=1}^{N} \frac{e^{jt}-a_n}{1-\overline{a}_n e^{jt}} \quad (6)$$

where $e_{\{a_n\}}(e^{jt})$ is called the evaluator at a_n which can be considered as a dictionary consisting of elementary functions [11]:

$$e_{\{a_n\}}(e^{jt}) = \frac{\sqrt{1-|a_n|^2}}{1-\overline{a}_n e^{jt}}. \quad (7)$$

According to (6), the energy of $G(t)$ can be calculated by [10]

$$\|G(t)\|^2 = \sum_{n=1}^{N} \left|\left\langle G_n, e_{\{a_n\}} \right\rangle\right|^2 + \left\|G_{N+1}(e^{jt})\right\|^2. \quad (8)$$

To make the energy of the standard remainder $\left\|G_{N+1}(e^{jt})\right\|^2$ minimum, the maximal projection principle shown in (9) is used to find a_n which can produce the largest $\left|\left\langle G_n, e_{\{a_n\}} \right\rangle\right|^2$ for every step n [10]. After getting the array $\{a_1, a_2, \cdots, a_n\}$, the main part of the AFD has been finished.

$$a_n = \arg\max \left\{ \left|\left\langle G_n, e_{\{a_n\}} \right\rangle\right|^2 : a_n \in \mathbb{D} \right\} \quad (9)$$

From the algorithm, we can see that there is a very large difference between the AFD and traditional decomposition methods. The AFD decomposes signals according to their energy distribution, making the AFD suitable for separating two parts whose frequency ranges overlap each other.

III. AFD-based Denoising Process

If the noise is not related with the original ECG signals, the noisy signal can be expressed by

$$f_{noise}(t) = f(t) + n(t) \quad (10)$$

where $f(t)$ and $n(t)$ are the pure signal and noise respectively, which is very similar with (1). The main technique of the AFD-based denoising process is to stop the recursive AFD process at a suitable decomposition level and reconstruct the filtered result using obtained mono-components [12]. At such suitable decomposition, the standard remainder contains most noise. Then the summation of the first N mono-components can be used to approximate the original pure signal. The approximation of the original signal can be expressed by

$$s_r(t) = 2\,\mathrm{Re}\left\{\tilde{G}\right\} - \left\langle G_1, e_{\{a_1\}} \right\rangle \quad (11)$$

where

$$\tilde{G}(t) = \sum_{n=1}^{N} \left\langle G_n, e_{\{a_n\}} \right\rangle B_n(e^{jt}). \quad (12)$$

To find the suitable decomposition level N, a judgment is defined based on the estimated SNR of the noisy signal. Since all decomposition components are from high-energy mode to low-energy mode, the judgment of the AFD can be defined by

$$\frac{\|s(t)\|^2}{2\sum_{n=1}^{N} \left|\left\langle G_n, e_{\{a_n\}} \right\rangle\right|^2 - \left|\left\langle G_1, e_{\{a_1\}} \right\rangle\right|^2} \le 1 + \frac{1}{10^{\mathrm{SNR}_e/10}} \quad (13)$$

where SNR_e is the estimated SNR of the noisy signal shown in decibel [12]. The recursive AFD process should be stopped once this judgment is reached. If the decomposition is continued, more noise will be included into the filtered result. If the decomposition process is stopped before (13) is reached, more energy of the original signal will be lost from the filtered result. The whole denoising process is shown in Alg. 1 [12].

Algorithm 1 Denoising procedure based on the AFD

Input: $s(t)$: noisy ECG signal; SNR_e: estimated SNR of $s(t)$

Initialize $a_1 = 0$, $N = 1$ and $G(t) = G_1(t) = s(t)$;

$e_{\{a_1\}}$ and $B_1 \leftarrow \frac{\sqrt{1-|a_1|^2}}{1-\overline{a}_1 e^{jt}}$;

$G_2 \leftarrow \left(G(t) - \left\langle G_1, e_{\{a_1\}}\right\rangle e_{\{a_1\}}\right) \frac{1-\overline{a}_1 e^{jt}}{e^{jt}-a_1}$;

$a_2 \leftarrow \arg\max \left\{ \left| \left\langle G_2, \frac{\sqrt{1-|a_2|^2}}{1-\overline{a}_2 e^{jt}} \right\rangle \right|^2 : a_2 \in \mathbb{D} \right\}$;

$e_{\{a_2\}} \leftarrow \frac{\sqrt{1-|a_2|^2}}{1-\overline{a}_2 e^{jt}}$;

$B_2 \leftarrow \frac{\sqrt{1-|a_2|^2}}{1-\overline{a}_2 e^{jt}} \frac{e^{jt}-a_1}{\sqrt{1-|a_1|^2}} B_1$; let $N = 2$;

$ER \leftarrow \frac{\|s(t)\|^2}{2\sum_{n=1}^{2} \left|\left\langle G_n, e_{\{a_n\}}\right\rangle\right|^2 - \left|\left\langle G_1, e_{\{a_1\}}\right\rangle\right|^2}$;

while $ER > 1 + \frac{1}{10^{\mathrm{SNR}_e/10}}$ **do**

  $G_{N+1} \leftarrow \left(G_N(t) - \left\langle G_N, e_{\{a_N\}}\right\rangle e_{\{a_N\}}\right) \frac{1-\overline{a}_N e^{jt}}{e^{jt}-a_N}$;

  $a_{N+1} \leftarrow \arg\max \left\{ \left| \left\langle G_{N+1}, \frac{\sqrt{1-|a_{N+1}|^2}}{1-\overline{a}_{N+1} e^{jt}} \right\rangle \right|^2 : a_{N+1} \in \mathbb{D} \right\}$;

  $e_{\{a_{N+1}\}} \leftarrow \frac{\sqrt{1-|a_{N+1}|^2}}{1-\overline{a}_{N+1} e^{jt}}$;

  $B_{N+1} \leftarrow \frac{\sqrt{1-|a_{N+1}|^2}}{1-\overline{a}_{N+1} e^{jt}} \frac{e^{jt}-a_N}{\sqrt{1-|a_N|^2}} B_N$; let $N = N+1$;

  $ER \leftarrow \frac{\|s(t)\|^2}{2\sum_{n=1}^{N} \left|\left\langle G_n, e_{\{a_n\}}\right\rangle\right|^2 - \left|\left\langle G_1, e_{\{a_1\}}\right\rangle\right|^2}$;

end while

$s_r \leftarrow 2\,\mathrm{Re}\left\{\sum_{n=1}^{N} \left\langle G_n, e_{\{a_n\}}\right\rangle B_n\right\} - \left\langle G_1, e_{\{a_1\}}\right\rangle$;

Output: s_r: reconstructed filtered result; N: final decomposition level

IV. Real Noise Simulation and Discussion

Simulations are carried out in the MATLAB environment using two types of ECG signals: artifact and real ECG signals. A combination of two types of real noise is added into these ECG signals. The artifact ECG signal is used to verify the denoising principle shown in section III, while some real ECG signals from the MIT-BIH Arrhythmia Database [14, 15] are used to compare filtered results using the AFD with the ones using the Butterworth lowepass filter, the wavelet transform and the EMD. The main AFD program is provided by Qian et al. [16].

A. Artifact ECG signal

The noise combination method is same as [17]. Two real noise records are taken from the MIT-BIH noise stress test database [15, 18], the muscle artifact "ma" record and the electrode motion "em" record. The baseline wander (BW) in each record is eliminated by lowpass filtering. The total noise is

$$n(t) = k_1 n_{\mathrm{ma}}(t) + k_2 n_{\mathrm{em}}(t) \tag{14}$$

where $n_{\mathrm{ma}}(t)$ and $n_{\mathrm{em}}(t)$ are the "ma" and "em" BW free noise records, respectively [17]. Moreover, k_1 and k_2 are chosen to contribute with the same SNR_0 [17]:

$$\mathrm{SNR}_0 = \frac{\sum_{t=0}^{L-1} x^2(t)}{\sum_{t=0}^{L-1} \left[k_1 n_{\mathrm{ma}}(t)\right]^2} = \frac{\sum_{t=0}^{L-1} x^2(t)}{\sum_{t=0}^{L-1} \left[k_1 n_{\mathrm{em}}(t)\right]^2}. \tag{15}$$

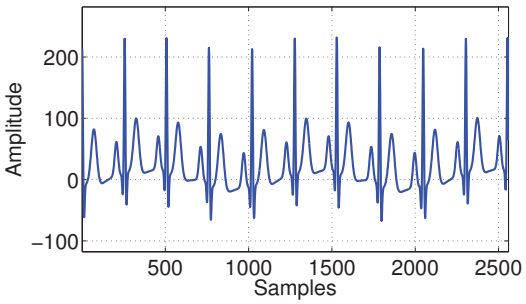

(a) Original clean artifact ECG signal.

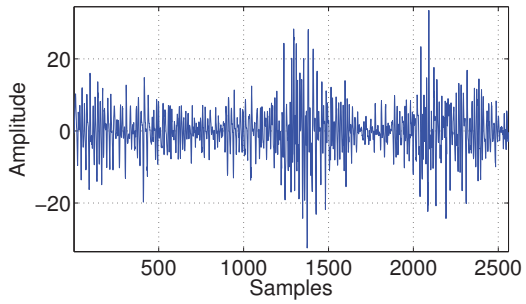

(b) 'ma' noise at 18dB.

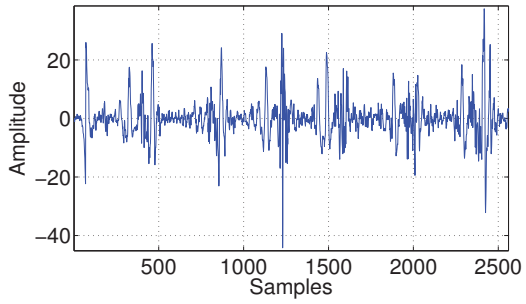

(c) 'em' noise at 18dB.

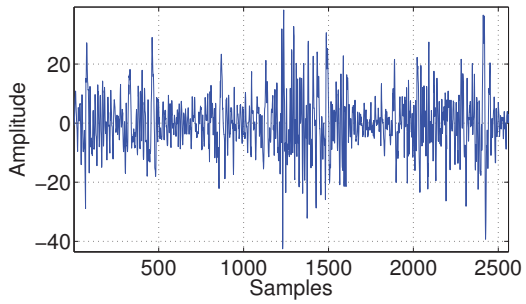

(d) Total noise at 14.88dB used to corrupt the original signal.

Fig. 1. Set of signals for the artifact ECG signal's simulation.

Fig. 1 shows the set of signals involved in this simulation of the artifact ECG signal. In Fig. 1(a), The first 2560 samples artifact ECG signal that is generated by a synthetic ECG generator is depicted. Detail of this model can be found in [19]. The sampling frequency is 256Hz. The heart rate is 60

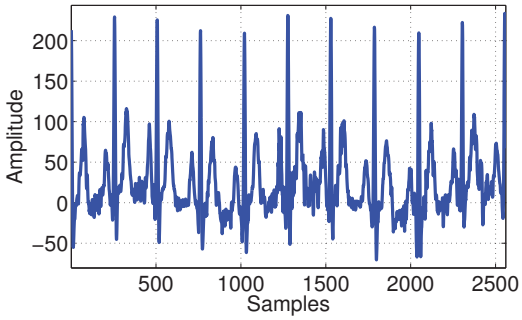

Fig. 2. Noisy ECG model signal with 14.88dB SNR.

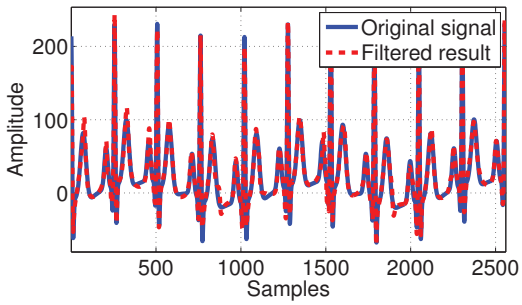

Fig. 3. Original ECG model signal and filtered result.

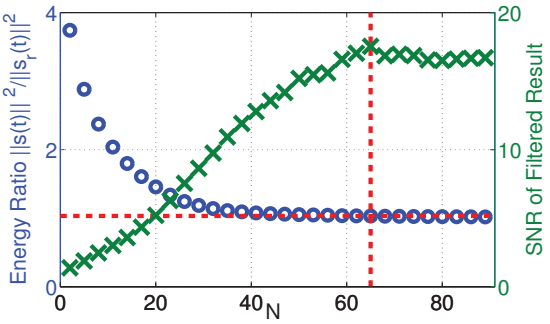

Fig. 4. Energy ratio of the noisy signal to the reconstructed ECG signal and SNR of the reconstructed ECG signal for different N.

beats per minutes. The noisy signal is obtained by adding the noise in Fig. 1(d) attaining an SNR of 14.88dB. The noise signal is obtained as the summation of "ma" noise and "em" noise in Fig. 1(b) and Fig. 1(c), respectively, at an SNR of 18dB in both cases. The noisy signal is shown in Fig. 2. After the AFD-based denoising method, the reconstructed filtered result can be obtained. Fig. 3 shows the reconstructed ECG signal with first 65 mono-components ($N = 65$) against the original clean ECG signal. Comparing these two signals shown in Fig. 3, it can be seen that the reconstructed signal almost reproduces the original ECG signal. In addition, the SNR of the reconstructed signal is increased to 17.54dB, which represents the improvement of 2.66dB to the noisy signal.

In Fig. 4, the cross symbol and circle symbol show the

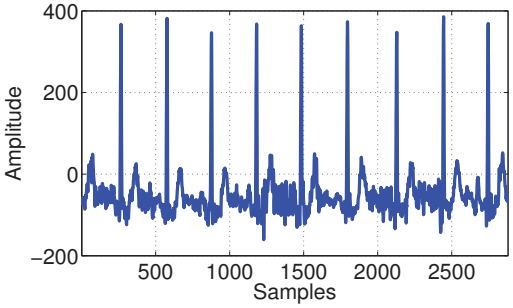

Fig. 5. Record 103 signal with real noise that makes the SNR 14dB.

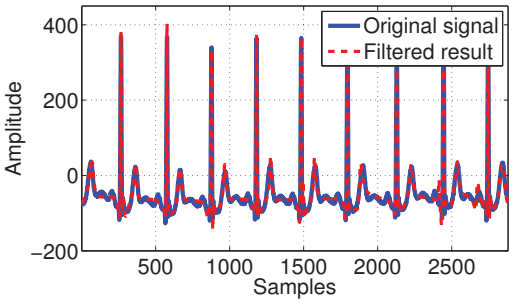

Fig. 6. Original 103 signal and reconstructed filtered result.

energy ratios of the energy of the noisy signals to the energy of the reconstructed filtered results and SNRs of reconstructed filtered results for different decomposition level N respectively. The horizontal dashed line shows the ideal energy ratio $1 + \frac{1}{10^{14.88/10}} = 1.03$. The vertical dashed line shows the optimal decomposition level $N = 65$ at which the SNR of the filtered result is maximum. According to Fig. 4, when the decomposition level increases, the energy ratio will decrease. In addition, the absolute value of the slope of the energy ratio will also decrease. At $N = 65$, it is the first time that the energy ratio is smaller than the ideal energy ratio. At the same time, the SNR of the filtered result also gets its maximum point. These observations validate the denoising principle of the AFD-based denoising method. Moreover, It shows that the AFD-based denoising method and the estimated-SNR-based judgment are able to be used to do real ECG noise reduction.

B. Real ECG signals

To evaluate the proposed denoising method, real ECG signals from the MIT-BIH Arrhythmia Database with the combination of real noise shown in Section IV-A are used to do the simulations. Fig. 5 shows the noisy record 103 signal with the combination of real noise that makes SNR 14dB. After using the proposed AFD-based denoising method, the filtered result shown in Fig. 6 can be obtained. Comparing the original record 103 signal and the filtered result shown in Fig. 6, the filtered result almost reproduces the original ECG signal. The AFD-based denoising method is able to improve the SNR of the noisy ECG signal.

TABLE I
PERFORMANCE (SNR) COMPARISON BETWEEN FILTERED RESULTS BASED ON THE EMD, THE WAVELET TRANSFORM AND THE AFD

Record No.	SNR = 6dB				SNR = 10dB				SNR = 14dB			
	SNR_{emd}	SNR_{butt}	SNR_{wt}	SNR_{AFD}	SNR_{emd}	SNR_{butt}	SNR_{wt}	SNR_{AFD}	SNR_{emd}	SNR_{butt}	SNR_{wt}	SNR_{AFD}
100	**11.40**	5.22	6.14	9.55	**13.95**	7.33	10.15	13.44	**16.75**	8.58	14.17	16.41
103	9.85	3.58	6.15	**10.34**	12.90	4.92	10.16	**13.43**	15.70	5.59	14.18	**16.37**
105	9.62	5.53	6.14	**10.88**	11.94	7.89	10.14	**12.76**	14.54	9.37	14.13	**16.28**
119	**11.45**	6.48	6.14	10.81	14.71	9.63	10.14	**14.75**	17.29	12.03	14.15	**17.81**
213	**8.87**	4.45	6.13	7.96	11.89	10.14	10.13	**12.00**	**14.74**	7.06	14.13	**14.74**

TABLE II
PERFORMANCE (SNR) UNDER DIFFERENT DECOMPOSITION LEVEL N

Record No.	SNR = 6dB			SNR = 10dB			SNR = 14dB		
	SNR_{se}	SNR_{op}	SNR_{diff}	SNR_{se}	SNR_{op}	SNR_{diff}	SNR_{se}	SNR_{op}	SNR_{diff}
100	9.55	10.12	0.57	13.44	13.56	0.12	16.41	16.99	0.58
103	10.34	11.20	0.86	13.43	13.75	0.32	16.37	17.08	0.71
105	10.88	10.89	0.01	12.76	13.16	0.40	16.28	16.93	0.65
119	10.81	11.44	0.63	14.75	14.77	0.02	17.81	18.05	0.24
213	7.96	8.82	0.86	12.00	12.69	0.69	14.74	15.67	0.93

To show the effectiveness of the AFD-based denoising method for real ECG noise reduction, three other denoising methods are used to compare with this AFD-based denoising method. These three methods are based on the Butterworth lowpass filter, the wavelet decomposition and the EMD. Their results are from [17]. In [17], 5 records' real ECG signals from the MIT-BIH Arrhythmia Database with the combination of real noise that makes SNR 6dB, 10dB and 14dB are used. We use the same records' signals and add the same type of noise to do this simulation. The comparing results are shown in TABLE I where SNR_{emd}, SNR_{butt}, SNR_{wt} and SNR_{AFD} denote the SNRs of the filtered results based on the EMD, the Butterworth lowpass filter, the wavelet transform and the AFD, respectively. It shows that the AFD-based denoising method almost performs better than the denoising method based on the EMD and the wavelet transform.

C. Discussion

Normally, the estimated-SNR-based judgment of the AFD-based denoising process provides the optimal decomposition level N. In simulations of real ECG signals, sometimes, the optimal decomposition level N and the provided N are not the same. According to the relationship between the energy ratio and the decomposition level N shown in Fig. 4, if the optimal decomposition level N and the provided N are large enough, and their difference is not very large, the performance of filtered results of these two cases should be almost same. The comparison of filtered performances between optimal N and provided N using 15 cases in section IV-B is shown in TABLE II where SNR_{se}, SNR_{op} and SNR_{diff} denotes the SNRs of filtered results of the selected N and the optimal N and the difference between SNR_{se} and SNR_{op}, respectively. It shows that the difference between the performances of the selected N and the optimal N is not very large. The filtered results of the selected decomposition level N are accepted.

$$|R_N| \leq \frac{M}{\sqrt{N}} \tag{16}$$

If we want to get optimal results, sometimes we still need to adjust the decomposition level after the proposed denoising process. From simulation results shown in section IV, some basic rules about choosing and adjusting the threshold of the AFD can be found. First, since the AFD is a kind of decompositions that is based on the energy. If the energy of noise is larger than the original signal, most of the reconstructed signal by using first several mono-components of the AFD will not be the original signal but the noise. In other words, it is not suitable for noisy signals whose SNRs are smaller than 0dB to use the proposed denoising method. Second, according to (1) and the relationship between decomposition level N and the energy of the standard remainder shown in (16) where M is defined by $\sum_{k=1}^{\infty} |c_k| \leq M$ [13], the relationship between the energy of the N-th mono-component and the threshold N can be found as

$$\|s_N(t)\|^2 \leq M^2 \left(\frac{1}{N} - \frac{1}{N+1} \right). \tag{17}$$

It shows that the energy of the N-th mono-component will decrease if the threshold N increases. The proposed decomposition method can be seen as a "high-energy pass filter". It will make sure that high-energy components will be decomposed first from the noisy signal. It implies that the final decomposition level N should be increased if we want to recover more energy. For denoising process, it means that the larger threshold N is needed to filter out noise from the noisy signal that has larger SNR. Third, different mono-components have different frequency ranges. If the basis function of the AFD is written by (4), it follows that

$$\phi_n'(t) < \phi_{n+1}'(t), \ t \in [0, 2\pi]. \tag{18}$$

It shows that the main frequency range of n-th mono-component will increase when n increases [20]. From this relationship, the proposed denoising method looks like a "lowpass filter". Therefore, the larger threshold N is needed to filter out noise from the noisy signal whose corresponding

original signal contains higher frequency components. These three rules can be used to determine and adjust the threshold of the denoising process of the AFD.

V. Conclusion

In [12], we proposed the AFD-based denoising method for filtering out the additive Gaussian white noise from ECG signals. This paper extends the method to the reduction of two types of real noise from ECG signals. These two types of real noise are added to the artifact and real ECG signals to test the performance of the AFD-based denoising method. The effectiveness of the AFD in ECG real noise denoising is shown through the tests on the MIT-BIH Arrhythmia Database. The AFD-based method mostly performs better than the methods based on the Butterworth lowpass filter, the EMD and the wavelet transform, showing that the AFD is a promising tool for ECG signal denoising. Moreover, three basic rules about how to choose and adjust the final decomposition level of the AFD are proposed, which can help users of the AFD-based denoising method to get the optimal filtered results.

Acknowledgment

This work is supported in part by the Macau Science and Technology Development Fund under grant FDCT 036/2009/A and the University of Macau Research Committee under grants MYRG139(Y1-L2)-FST11-WF, MYRG079(Y1-L2)-FST12-VMI, MYRG069(Y1-L2)-FST13-WF and MYRG2014-00174-FST.

References

[1] M. Alfaouri and K. Daqrouq, "ECG signal denoising by wavelet transform thresholding," *Amer. J. Appl. Sci.*, vol. 5, no. 3, 2008.

[2] P. Tikkanen, "Nonlinear wavelet and wavelet packet denoising of electrocardiogram signal," *Biol. Cybern.*, vol. 80, no. 4, pp. 259–267, 1999.

[3] O. Sayadi and M. B. Shamsollahi, "ECG denoising with adaptive bionic wavelet transform," in *Proc. IEEE Conf. Eng. Med. Biol. Soc.*, 2005, pp. 6597–6600.

[4] E. Ercelebi, "Electrocardiogram signals de-noising using lifting-based discrete wavelet transform," *Comput. Biol. Med.*, vol. 34, no. 6, pp. 479–493, 2004.

[5] G. U. Reddy, M. Muralidhar, and S. Varadarajan, "ECG de-noising using improved thresholding based on wavelet transforms," *Int. J. Inf. Comput. Secur.*, vol. 9, no. 9, pp. 221–225, 2009.

[6] B. Weng, M. Blanco-Velasco, and K. E. Barner, "ECG denoising based on the empirical mode decomposition," in *Proc. of the 28th IEEE Int. Conf. on EMBS*, New York, USA, 2006, pp.1–4.

[7] K. M. Chang and S. H. Liu, "Gaussian noise filtering from ECG by Wiener filter and ensemble empirical mode decomposition," *J. Sign. Process. Syst.*, vol. 64, no. 2, pp. 249–264, 2011.

[8] T. Qian, Y. B. Wang, and P. Dang, "Adaptive decomposition into mono-components," *Adv. Adapt. Data Anal.*, vol. 1, no. 04, pp. 703–709, 2009.

[9] R. C. Sharpley and V. Vatchev, "Analysis of the intrinsic mode functions," *Constr. Approx.*, vol. 24, no. 1, pp. 17–47, 2006.

[10] T. Qian, L. M. Zhang, and Z. X. Li, "Algorithm of adaptive fourier decomposition," *IEEE Trans. Signal Process.*, vol. 59, no. 12, pp. 5899–5906, 2011.

[11] T. Qian and Y. B. Wang, "Adaptive decomposition into basic signals of non-negative instantaneous frequencies - a variation and realization of greedy algorithm," *Adv. Comput. Math.*, vol. 34, no. 3, pp. 279–293, 2011.

[12] Z. Wang, C. M. Wong, J. N. da Cruz and F. Wan, "Adaptive Fourier decomposition approach for ECG signal denoising," unpublished.

[13] T. Qian and Y. Wang, "Remarks on adaptive Fourier decomposition," *Int. J. Wavelets Multi.*, vol. 11, no. 1, 2013.

[14] G. B. Moody and R. G. Mark, "The impact of the MIT-BIH Arrhythmia Database," *IEEE Eng. Med. Biol. Mag.*, vol. 20, no. 3, pp. 45–50, May-June 2001.

[15] A. L. Goldberger, L. A. N. Amaral, L. Glass, J. M. Hausdorff, P. C. Ivanov, R. G. Mark, J. E. Mietus, G. B. Moody, C. K. Peng, and H. E. Stanley, "PhysioBank, PhysioToolkit, and PhysioNet: Components of a new research resource for complex physiologic signals," *Circulation*, vol. 101, no. 23, pp. e215–e220, June 13 2000.

[16] T. Qian and W. X. Mai. (2012, Jan. 10). *AFDs software* [Online]. Available: http://www.fst.umac.mo/en/staff/documents/fsttq/afd_form/index.html.

[17] M. Blanco-Velasco, B. Weng and K. E. Barner, "ECG signal denoising and baseline wander correction based on the empirical mode decomposition," *Comput. Biol. Med.*, vol. 38, no. 1, pp. 1–13, 2008.

[18] G. B. Moody, W. E. Muldrow and R. G. Mark, "A noise stress test for arrhythmia detectors," *Comput. Cardiol.*, vol. 11, no. 3, pp. 381–384, 1984.

[19] P. E. McSharry, G. D. Clifford, L. Tarassenko, and L. A. Smith, "A dynamical model for generating synthetic electrocardiogram signals," *IEEE Trans. Biomed. Eng.*, vol. 50, no. 3, pp. 289–294, 2003.

[20] P. Dang, T. Qian, and Y. Y. Guo, "Transient time-frequency distribution based on mono-component decompositions," *Int. J. Wavelets Multi.*, vol. 11, no. 3, 2013.